
レーザーアニールによるPZT薄膜の結晶化技術の開発

Development of Crystallization of PZT Films by Laser Annealing

陳 顕鋒*
Xianfeng CHEN

八木 雅広*
Masahiro YAGI

要 旨

ゾルゲル法で作製したチタン酸ジルコン酸鉛 (PZT) アモルファス膜を、波長980nm半導体レーザーで下部電極の白金 (Pt) 部を加熱して結晶化させることを我々は討議した。膜の比誘電率測定により1回のレーザーアニール処理で厚さ45nmのPZT結晶膜を形成できることが分かった。このため、毎回塗布した膜の厚みを45nm以下に抑え、かつレーザーアニールパワーを制御することで、厚さ150nmPZT結晶膜を4回繰返して成膜した。得られたPZT膜の比誘電率は1,200、圧電定数は従来のラピッドサーマルアニール (RTA) 法で結晶化したPZT膜と同等レベルを達成した。

ABSTRACT

Crystallization of $\text{Pb}(\text{Zr}_{0.53}\text{Ti}_{0.47})\text{O}_3$ (PZT) films, derived from PZT sol-gel solutions, using a continuous-wave (CW) 980 nm semiconductor laser is discussed in this paper. From dielectric constant measurement, it is found that one laser annealing (LA) process generates 45-nm-thick crystallized PZT layer. By using 0.3 M precursor solution and repeating 4 times the LA processes, 150-nm-thick crystallized PZT films are obtained with (111)-preferred texture. By adjusting the laser power for each annealing process, PZT crystallization is formed in the entire film, which is confirmed by electron diffraction patterns. The dielectric constant of the PZT film is about 1200. Its longitude piezoelectric constant (d_{33}), measured by an atomic force microscopy, is comparable to that of PZT film fabricated by rapid thermal annealing.

* GJ開発本部 GC開発センター
GC Development Center, GJ Design & Development Division

1. Introduction

$\text{Pb}(\text{Zr}_{0.53}\text{Ti}_{0.47})\text{O}_3$ (PZT) has excellent piezoelectric properties and is extensively used in various devices, including print heads of inkjet printers. PZT films can be fabricated by sol-gel (SG) deposition, sputtering, and so forth. Compared with other methods, SG method offers several advantages, such as precise stoichiometry control, low cost, and large surface coverage. Therefore, it is widely adopted in PZT industrial fabrication.

To crystallize PZT films derived from SG solution, a thermal annealing process is necessary. It is generally carried out by heating up the sample to about 750 °C in a rapid thermal annealing (RTA) apparatus, where almost all heat energy is used to raise and lower the temperature of the substrate and the apparatus body, resulting in significant waste of heat energy and run time. Laser annealing (LA) is an efficient annealing technique that it can only heat the wanted areas by selecting right wavelength and has been used in manufacture of solar cells and power devices.

Many researchers have attempted to apply this technique to PZT crystallization since three decades ago¹⁻⁷⁾. To date, only Baba et al.⁶⁾, who used a CO₂ laser, and Bharadwaja et al.⁷⁾, who used an excimer laser, reported that they obtained crystallized LA-PZT films as good as RTA-treated ones. However, in these cases, particular amorphous PZT films were preformed.

Considering productivity, a semiconductor diode laser is preferred because of its low cost, small size, and low energy consumption, compared with conventional solid state, CO₂ or excimer lasers. In this paper, we provide a method that can be used to crystallize PZT films derived from SG solution on Pt-metalized Si substrate by LA treatment. Characteristics of the LA-PZT films are also reported.

2. Experimental

The laser used for the annealing treatment is a 980 nm continuous-wave (CW) semiconductor laser. It has a maximum output power of 300 W. Part of the laser annealing system is shown in Fig.1. The laser irradiation beam is modified to a rectangular shape (1000 X 350 μm^2) with a flat-top intensity profile.

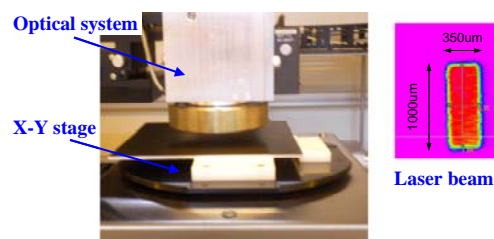


Fig.1 Laser annealing system used in the experiment.

Two kinds of PZT SG solutions synthesized in a 2-methoxyethanol based route are used in the experiment. The solutions have the same composition, where Zr/Ti ratio is 53/47 and Pb excess is 10.8%, but they have different concentrations. One solution has a concentration of 0.5 M, and the other has a concentration of 0.3 M. The 0.5 M solution was used to calculate the possible thickness of crystallized PZT by one LA process, the 0.3 M solution was used to generate well-crystallized PZT films.

A flow chart of the LA process is shown in Fig.2. After spin-coating the PZT precursor solution on a Pt-metalized Si substrate at a speed of 3000 rpm for 20 s, the wafer was dried at 120 °C for 1 min and pyrolyzed at a temperature of 200 °C for 1 min to form amorphous PZT. Then, LA treatment was carried out at room temperature in an atmospheric environment by setting the wafer on an X-Y stage and scanning the laser beam on the wafer surface along the 350 μm side at a speed of 10 mm/s. To get thick PZT films, this process is repeated, until the desired thickness is achieved.

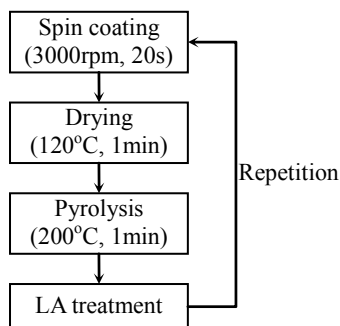


Fig.2 Flow chart of the LA process.

After that, a Pt upper electrode of 200 μm diameter was sputter-deposited in the LA-PZT area through a shadow mask to evaluate the electrical properties.

X-ray diffraction (XRD; PANalytical X'Pert Pro) and transmission electron microscopy (TEM; Hitachi N-9000NAR) were carried out to assess the crystal characteristics of LA-PZT films. The dielectric constant and loss tangent were measured using an impedance analyzer (HP4194A). The field-induced strain properties were evaluated using a ferroelectric test system (Toyo Technica FCE-1) and an atomic force microscopy (AFM; SPA-400) equipment.

3. Results and Discussion

Since the photon energy of the 980 nm laser is much less than the band gap energy of PZT, the laser energy will be mainly absorbed by the Pt lower electrode and converted to heat there, but little in PZT films. Therefore, when the thickness of PZT films is changed, the scanning laser output power has to be adjusted to keep the heat generation rate in the Pt films at a certain value.

Fig.3 shows the XRD pattern of a LA-PZT sample derived from the 0.5 M PZT precursor solution by repeating 2 times the LA processes on a Pt(111)/Si substrate. The laser powers used for the first and second LA treatments are 55 and 100 W, respectively. The XRD pattern reveals that the amorphous PZT was crystallized

with a (111)-preferred orientation. For the RTA process, it is usually argued that the PZT texture is determined by the transient intermediate layer formed on Pt at the initial annealing stage⁸⁻¹⁰. However, it is also considered that the strain generated in the PZT film affects its texture^{11,12}. As the LA treatment is different from the RTA treatment and has only millisecond-order duration, the crystallization mechanism is not clear yet.

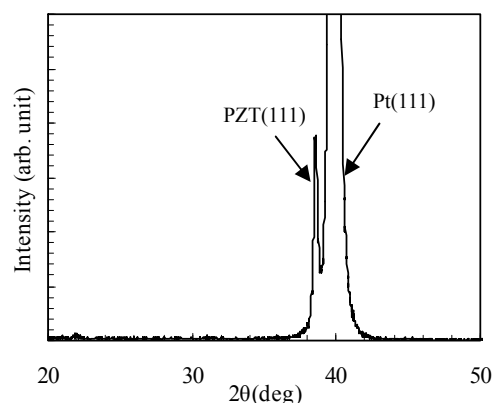


Fig.3 XRD pattern of a double layer LA-PZT film.

To determine the thickness of crystallized PZT film by one LA treatment, a two-layer PZT sample is prepared. Its schematic structure is shown in Fig.4. LA treatment was only performed to part of the first layer. The thickness of the areas with (Fig.4 (a)) and without (Fig.4 (b)) LA treatment are 125 and 132 nm, respectively. The thickness difference is considered to be caused by the shrinkage of the PZT film, when it is changed from amorphous to crystalline phase. Since heat is generated in the Pt lower electrode, PZT crystallization is estimated to start near it and then extends to the upper part.

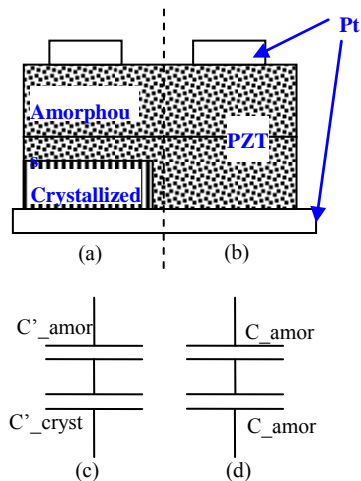


Fig.4 Schematic structure of a two-layer PZT film.

The measured dielectric constant ($\text{osc} = 0.8 \text{ V}$ at 10 kHz) of PZT in Fig.4 (a) is 80, while that in Fig.4 (b) is 50. As the dielectric constant of the crystallized PZT is assumed to be 1300^{13} , using the models shown in Figs.4 (c) and (d), it can be calculated that the thickness of the crystallized PZT layer in Fig.4 (a) is about 45 nm. Thus, reducing the thickness of each deposited PZT layer is a possible method of fabricating well-crystallized thick PZT films by the LA treatment.

A 150-nm-thick PZT film was obtained by using 0.3 M SG solution and repeating 4 times the LA processes. The laser power was adjusted for each LA process. A cross-sectional dark field TEM image of the sample is shown in Fig.5. Although it is a four-layer sample, the interface lines are not clear. This is attributed to the low pyrolysis temperature used in the LA process and short annealing duration, which prevented the Pb evaporation. The inserted figure shows an electron diffraction pattern of the PZT film. The incident electron beam is about 100 nm in diameter, which is close to the PZT film thickness. Thus, the ordered dot-pattern indicates that the entire film is well crystallized. The measured dielectric constant of the LA-PZT film, which is about 1200, can also demonstrate it.

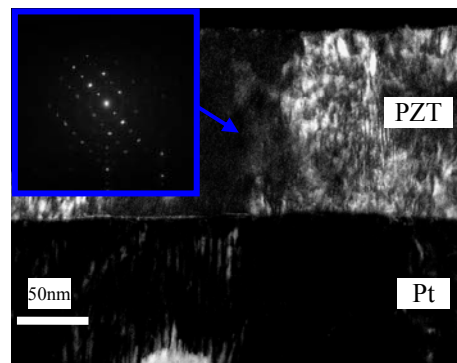


Fig.5 Cross-sectional dark field TEM image of the 150-nm-thick LA-PZT film.

The displacement-voltage ($\delta\text{-V}$) results measured by the AFM method at a driving frequency of 3 Hz are shown in Fig.6. For the LA-PZT, Fig.6 (a) shows that calculated longitudinal piezoelectric constant (d_{33}) in positive sweep loop (d_{33+}) is 61 pm/V and that in the negative sweep loop (d_{33-}) is 113 pm/V. A RTA-PZT sample was also measured by the same form. The result is shown in Fig.6 (b), where its d_{33+} and d_{33-} are 60 and 101 pm/V, respectively. The AFM evaluation suggests that the LA-PZT film has piezoelectric properties comparable to those of the RTA-PZT film. The poor appearance of the $\delta\text{-V}$ curves of LA-PZT might result from the thin film thickness. Because the absolute displacement is small, noise interference is relatively larger. Especially, when the driving voltage is near to 0, the displacement is too small to be detected correctly.

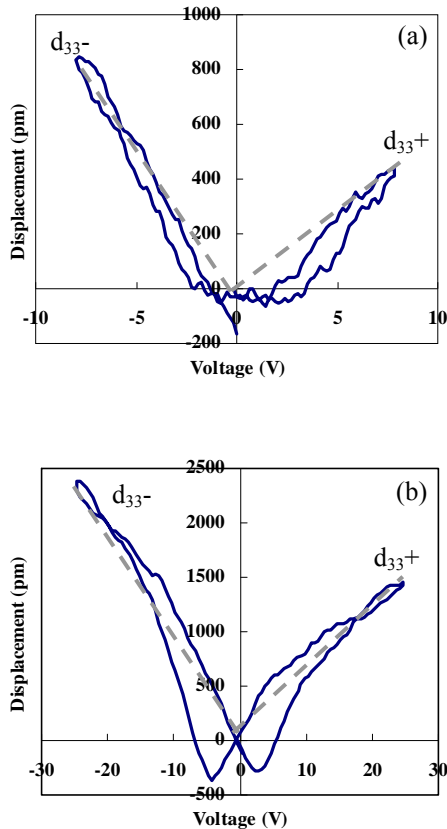


Fig.6 Displacement-voltage behaviors of (a) LA-PZT and (b) RTA-PZT films.

4. Conclusions

Using a 980 nm CW semiconductor laser, we have developed PZT films in an atmospheric environment. By controlling thickness of each deposition layer and adjusting the corresponding laser output power, well-crystallized 150-nm-thick LA-PZT films are obtained. The films show good piezoelectric properties comparable to those of RTA-PZT films. The LA process could save not only the energy but also the process time. In addition, together with the inkjet printing (IJP) technique, which could eject droplets of PZT SG solution in selected areas¹⁴⁾, the LA technique can easily integrate piezoelectric devices with others and is expected to open a new field of PZT application.

Acknowledgements

The authors would like to thank Professor H. Funakubo of Tokyo Institute of Technology for the measurement of the piezoelectric constant.

References

- 1) Y. Matsui, et al.: Laser annealing to produce ferroelectric-phase PbTiO₃ thin films, *J. Appl. Phys.*, Vol.52, pp.5107-5111 (1981).
- 2) X. M. Lu, et al.: Pulsed excimer (KrF) laser induced crystallization of PbZr_{0.44}Ti_{0.56}O₃ amorphous films, *Appl. Phys. Lett.*, Vol.66, pp.2481-2483 (1995).
- 3) P. P. Donohue and M. A. Todd: Pulse-extended excimer laser annealing of lead zirconate titanate thin films, *Integrated Ferroelectrics*, Vol.31, pp.285-296 (2000).
- 4) H. -C. Pan, et al.: Low-temperature processing of sol-gel derived La_{0.5}Sr_{0.5}MnO₃ buffer electrode and PbZr_{0.52}Ti_{0.48}O₃ films using CO₂ laser annealing, *Appl. Phys. Lett.*, Vol.83, pp.3156-3158 (2003).
- 5) S. C. Lai, et al.: Extended-pulse excimer laser annealing of Pb(Zr_{1-x}Ti_x)O₃ thin film on LaNiO₃ electrode, *J. Appl. Phys.*, Vol.96, pp.2779-2784 (2004).
- 6) S. Baba, et al.: Effect of carrier gas species on ferroelectric properties of PZT/Stainless-Steel fabricated by CO₂ laser-assisted aerosol deposition, *J. Am. Ceram. Soc.*, Vol.89, pp.1736-1738 (2006).
- 7) S. S. N. Bharadwaja, et al.: Highly textured laser annealed Pb(Zr_{0.52}Ti_{0.48})O₃ thin films, *Appl. Phys. Lett.*, Vol.99, 042903 (2011).
- 8) T. schneller, et al.: Investigation of the amorphous to crystalline phase transition of chemical solution deposited Pb(Zr_{0.3}Ti_{0.7})O₃ thin films by soft X-ray absorption and soft X-ray emission spectroscopy, *J. Sol-Gel Sci. Technol.*, Vol.48, pp.239-252 (2008).

- 9) U. Ellerkmann, et al.: Reduction of film thickness for chemical solution deposited $\text{PbZr}_{0.3}\text{Ti}_{0.7}\text{O}_3$ thin films revealing no size effects and maintaining high remanent polarization and low coercive field, *Thin Solid Films*, Vol.516, pp.4713-4719 (2008).
- 10) S. Y. Chen and I. W. Chen, Temperature-time texture transition of $\text{Pb}(\text{Zr}_{1-x}\text{Ti}_x)\text{O}_3$ thin films: I, Role of Pb-rich intermediate phases, *J. Am. Ceram. Soc.*, Vol.77, pp.2332-2336 (1994).
- 11) S. Y. Chen and I. W. Chen, Texture development, microstructure evolution, and crystallization of chemically derived PZT thin films, *J. Am. Ceram. Soc.*, Vol.81, pp.97-105 (1998).
- 12) J. H. Lee, et al.: Microstress relaxation effect of $\text{Pb}(\text{Zr}_{0.52}\text{Ti}_{0.48})\text{O}_3$ films with thickness for micro/nanopiezoelectric device, *Appl. Phys. Lett.*, Vol.96, 092904 (2010).
- 13) T. Ijima, et al.: Synthesis of 10- μm -thick lead zirconate titanate films on 2-in. Si substrates for piezoelectric film devices, *Int. J. Appl. Ceram. Technol.*, Vol.3, pp.442-447 (2006).
- 14) O. Machida, et al.: Fabrication of lead zirconate titanate films by inkjet printing, *Jpn. J. Appl. Phys.*, Vol.51, 09LA11 (2012).